Efficiency Enhancement of a Three Phase Soft Switching Inverter Under Light Load Conditions

Khaled A. Mahafzah, Klaus Krischan, Annette Muetze, *Fellow, IEEE*
Electric Drives and Machines Institute
Graz University of Technology, 8010 Graz, Austria
khaled.mahafzah@tugraz.at, klaus.krischan@tugraz.at, muetze@tugraz.at

***Abstract*—This paper studies the performance of a three phase Soft Switching Inverter (SSI) under extremely light load conditions (7 W, 150 mA-peak, 50 V-peak which is 10 % of its thermally maximum permissible power). An Auxiliary Resonant Commutated Pole Inverter (ARCPI) has been selected as soft switching topology for this research. Analytic approaches are used to compute the losses and to select the power transistor which best fits this application. Two options to enhance the efficiency are discussed. First, the switching losses of the auxiliary switches are reduced by optimizing the turn on and off sequence. Second, a Resonant Gate Drive (RGD) is employed to reduce the gate losses of the switches. A single phase prototype has been realized. Measurements and computed losses are compared to validate the model and the calculations.**

I. Introduction

In industrial applications, the energy conversion efficiency of power electronics systems is commonly a central theme. Targeting efficiency requires consideration of all the losses in the power circuit. The losses are commonly divided into three components: conduction, switching and gate losses [1].

Soft switching topologies (resonant inverters) have been used widely because of their inherent ability to reduce the switching losses that are typically of significant influence in hard switching inverters. In [2]-[5], different resonant circuits have been discussed in detail.

Many researchers studied the Auxiliary Resonant Commutated Pole Inverter (ARCPI) with relatively high loads: in [6], the operation of an ARCPI is reviewed and the losses are estimated analytically. In [7], the design of an ARCPI is discussed in more detail for an AC drive as the target application. In [8], an ARCPI has been designed for a 3.3 hp brushless DC motor drive system.

This paper studies the performance of a conventionally Pulse Width Modulation (PWM) controlled Soft Switching Inverter (SSI) designed for a low power application. As the rated power of 70 W, 310 mA-peak and 260 V-peak is only required a few times during its lifetime, it is not relevant for the energy consumption of the appliance. The converter must operate at 7 W, which is 10 % of the maximum load, for most of the time. A hard switching approach to this load has been proposed in [19]. Thus, this study has been carried out based on the partial load point (7 W, 150 mA-peak, 50 V-peak) which is the most frequent operation point to be expected. (Any possible output filter is excluded from the study, since, if needed at all, it would depend on the length of the cable used.)

Section II discusses the analytic approach to compute the losses. The selection of the components of the circuit is discussed in Section III. Some options to improve the efficiency of the inverter are discussed in Section IV. Test circuit, set up, measurements and model validation are discussed in Section V. Finally, conclusions are drawn in Section VI.

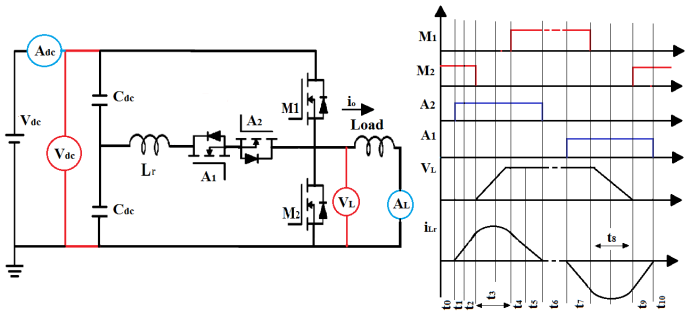

Fig. 1. Single leg, Auxiliary Resonant Commutated Pole (left), Gating sequence (M_1,M_2 for main switches. A_1, A_2 for auxiliary switches), load voltage (V_L) and inductor current (i_{Lr}) (right), [2].

II. ARCPI Losses Analysis

This section computes the loss components for a single leg of the ARCPI because the three phase inverter is composed of three identical legs and operated with a symmetrical load. This single leg is reviewed in Figure 1 (left).

In the analysis, the following nomenclature is used for the MOSFETs and the IGBTs which may be used both as main and auxiliary switches:

- R_{on} denotes the on-state resistances, for the MOSFETs (R_{dson}) and the differential resistance for the IGBTs (R_{ce}). R_L symbolizes the internal DC resistance of the inductor.
- The voltage across the semiconductor device (diode or the channel of the switch) is symbolized by V_x. It is a combination of the on voltage at zero current plus the multiplication of the differential resistance and the current (I_x) passing through the device. (V_f+$R_f I_x$ for diodes, V_{ce}+$R_{ce} I_x$ for IGBTs and $0 + R_{dson} I_x$ for MOSFETs.)
- The current drawn by the load in the n-th switching cycle is denoted $i_{o\text{-}n}$.

Further, the following assumptions are made:

- As long as $i_{\text{o-n}} R_{\text{on}} < V_{\text{f}}$, the body diode will not conduct but the channel of the MOSFET will do so if it is gated on.
- For the computations in Section III, the boost inductor current is assumed to be three and half times the peak of the load current, where $I_{\text{b-n}} = 3.5 i_{\text{o-peak}}$.
- The equations in the following section are based on the homogeneous ARCPI using MOSFETs only, but can easily be extended for IGBTs.

The current drawn by the load is symmetrical in the positive and the negative half cycles of the fundamental period ($f_{\text{mod}} = 50\,\text{Hz}$), so the energy losses are calculated for the positive half wave only. Then, twice of these are averaged over one fundamental period.

A. ARCPI Operating Sequences

The ACRCPI has ten operating sequences within one switching period [2,6,7]. Figure 1 (right) reviews the switching pattern for all the switches with the load voltage and inductor current during one switching cycle, assuming the positive load current flows out of the inverter. Table I summarizes the conducting semiconductors in each sequence. Table II shows the resistance values and the driving voltages for the resonant inductor current differential equations.

- Sequence 1, period t_1: The lower main switch (M_2) and both auxiliary switches (A_1, A_2) are gated on. M_2 and A_2 are conducting in reverse direction and (A_1) is conducting in forward direction. Applying Kirchhoff's voltage law (KVL) through the loop results in:

$$\frac{-V_{\text{dc}}}{2} + V_{\text{xa2}} + V_{\text{xa1}} + I_{\text{L1}} R_{\text{L}} + L\frac{dI_{\text{L1}}}{dt} - V_{\text{xm2}} = 0 \quad (1)$$

Rearranging this equation yields:

$$L\frac{dI_{\text{L1}}}{dt} + R_{\text{t1}} I_{\text{L1}} = V_{\text{t1}} \quad (2)$$

According to assumption no. 1, the body diodes of A_2 and M_2 will not conduct so that R_{t1} and V_{t1} are found (in switching cycle number n), as summarized in Table II:

$$R_{\text{t1}} = R_{\text{L}} + 2R_{\text{ona}} + R_{\text{onm2}} \quad (3)$$

$$V_{\text{t1-n}} = \frac{V_{\text{dc}}}{2} + V_{\text{xm2}} \quad (4)$$

Eq. (2) is a first order differential equation, with the initial condition $I_{\text{L}}(t_{1\text{i}}) = 0$ and the final condition $I_{\text{L}}(t_{1\text{f-n}}) = i_{\text{o-n}}$. Solving for the inductor current yields:

$$I_{\text{L1-n}} = \frac{V_{\text{t1-n}}}{R_{\text{t1}}}\left(1 - e^{\frac{-R_{\text{t1}}}{L}t}\right) \quad (5)$$

Then, sequence 1 has the duration of:

$$t_{\text{1-n}} = \frac{-L}{R_{\text{t1}}} \ln\left(1 - R_{\text{t1}}\frac{i_{\text{o-n}}}{V_{\text{t1-n}}}\right) \quad (6)$$

- Sequence 2, period t_2: The initial and final conditions are $I_{\text{L}}(t_{2\text{i-n}}) = i_{\text{o-n}}$ and $I_{\text{L}}(t_{2\text{f-n}}) = I_{\text{b-n}}$. Then, solving for the inductor current yields:

$$I_{\text{L2-n}} = \frac{V_{\text{t2-n}}}{R_{\text{t2}}} + \left(i_{\text{o-n}} - \frac{V_{\text{t2-n}}}{R_{\text{t2}}}\right) e^{\frac{-R_{\text{t2}}}{L}t} \quad (7)$$

Sequence 2 has the duration of:

$$t_{\text{2-n}} = \frac{-L}{R_{\text{t2}}} \ln\left(\frac{I_{\text{b-n}} - \frac{V_{\text{t2-n}}}{R_{\text{t2}}}}{i_{\text{o-n}} - \frac{V_{\text{t2-n}}}{R_{\text{t2}}}}\right) \quad (8)$$

- Sequence 3, period t_3: This is the first resonant mode per switching cycle with the inductor and the combination of non-linear output capacitances of the main switches and the constant load capacitance (all capacitances are acting in parallel). Applying KVL yields:

$$\frac{-V_{\text{dc}}}{2} + V_{\text{xa2}} + R_{\text{L}} I_{\text{L3}} + L\frac{dI_{\text{L3}}}{dt} + V_{\text{Cm}} = 0 \quad (9)$$

V_{Cm} is obtained by:

$$V_{\text{Cm}} = \frac{1}{2C_{\text{m}} + C_{\text{load}}} \int (I_{\text{L3}} - i_{\text{o-n}}) dt \quad (10)$$

Finding the first derivative of (9) and rearranging the terms yields:

$$L\frac{dI^2_{\text{L3-n}}}{dt^2} + R_{\text{t3}}\frac{dI_{\text{L3-n}}}{dt} + \frac{I_{\text{L3-n}} - i_{\text{o-n}}}{2C_{\text{m}} + C_{\text{load}}} = 0 \quad (11)$$

where R_{t3} is shown in Table II.
This is a second order differential equation with the initial and final conditions $I_{\text{L3-n}}(t_{3i-n}) = I_{\text{b-n}}$, the output capacitance of the switch initial voltage $V_{\text{Ci3-n}} = V_{\text{onm}} + R_{\text{onm}}(I_{\text{b-n}} - i_{\text{o-n}})$ and the final voltage of this capacitor $V_{\text{Cf3}} = V_{\text{dc}} + V_{\text{fm2}}$. From the characteristic equation of (11):

$$\delta_3 = \frac{R_{\text{t3}}}{2L} \quad (12)$$

$$\omega_3 = \sqrt{-\delta_3^2 + \frac{1}{L(2C_{\text{m}} + C_{\text{load}})}} \quad (13)$$

$$\lambda_{13,23} = -\delta_3 + j\omega_3, -\delta_3 - j\omega_3 \quad (14)$$

Solving for the inductor current during the resonance mode yields:

$$I_{\text{L3-n}} = (2C_{\text{m}} + C_{\text{load}})\, e^{-\delta_3 t}(\lambda_{13} A_{3\text{-n}} e^{j\omega_3 t} + \lambda_{23} B_{3\text{-n}} e^{-j\omega_3 t}) + i_{\text{o-n}} \quad (15)$$

where:

$$A_{3\text{-n}} = \frac{I_{\text{b-n}} - i_{\text{o-n}} - (2C_{\text{m}} + C_{\text{load}})\lambda_{23}(V_{\text{Ci3-n}} - 0.5V_{\text{dc}} + R_{\text{t3}} i_{\text{o-n}})}{2j\omega_3(2C_{\text{m}} + C_{\text{load}})} \quad (16)$$

$$B_{3\text{-n}} = \frac{-I_{\text{b-n}} + i_{\text{o-n}} + (2C_{\text{m}} + C_{\text{load}})\lambda_{13}(V_{\text{Ci3-n}} - 0.5V_{\text{dc}} + R_{\text{t3}} i_{\text{o-n}})}{2j\omega_3(2C_{\text{m}} + C_{\text{load}})} \quad (17)$$

The duration of this sequence is given by:

$$t_{3\text{-n}} = \frac{\ln\left(\frac{(V_{\text{Cf3}} - 0.5V_{\text{dc}})}{2A_{3\text{-n}}} + \sqrt{\frac{(V_{\text{Cf3}} - 0.5V_{\text{dc}})^2}{4A^2_{3\text{-n}}} - \frac{B_{3\text{-n}}}{A_{3\text{-n}}}}\right)}{j\omega_3} \quad (18)$$

- Sequence 4, period t_4: Solving for the inductor current with the initial and final conditions of $I_{\text{L4}}(t_{4\text{i-n}}) = I_{\text{b-n}}$

(the losses during the resonant period, lowering the current below I_{b} are neglected) and $I_{\mathrm{L4}}(t_{\mathrm{4f\text{-}n}}) = i_{\mathrm{o\text{-}n}}$ yields:

$$I_{\mathrm{L4\text{-}n}} = \frac{V_{\mathrm{t4\text{-}n}}}{R_{\mathrm{t4}}} + \left(I_{\mathrm{b\text{-}n}} - \frac{V_{\mathrm{t4\text{-}n}}}{R_{\mathrm{t4}}}\right) e^{-\frac{R_{\mathrm{t4}}}{L}t} \tag{19}$$

where R_{t4} and V_{t4} are shown in Table II. The duration of this sequence is given by:

$$t_{\mathrm{4\text{-}n}} = \frac{-L}{R_{\mathrm{t4}}} \ln\left(\frac{i_{\mathrm{o\text{-}n}} - \frac{V_{\mathrm{t4\text{-}n}}}{R_{\mathrm{t4}}}}{I_{\mathrm{b\text{-}n}} - \frac{V_{\mathrm{t4\text{-}n}}}{R_{\mathrm{t4}}}}\right) \tag{20}$$

- Sequence 5, period t_5: The initial and final conditions are $I_{\mathrm{L5}}(t_{\mathrm{5i\text{-}n}}) = i_{\mathrm{o\text{-}n}}$ and $I_{\mathrm{L5}}(t_{\mathrm{5f\text{-}n}}) = 0$. The inductor current is given by:

$$I_{\mathrm{L5\text{-}n}} = \frac{V_{\mathrm{t5\text{-}n}}}{R_{\mathrm{t5}}} + \left(I_{\mathrm{b\text{-}n}} - \frac{V_{\mathrm{t5\text{-}n}}}{R_{\mathrm{t5}}}\right) e^{-\frac{R_{\mathrm{t5}}}{L}t} \tag{21}$$

Then, the duration of this sequence is given by:

$$t_{\mathrm{5\text{-}n}} = \frac{-L}{R_{\mathrm{t5}}} \ln\left(\frac{\frac{-V_{\mathrm{t5\text{-}n}}}{R_{\mathrm{t5}}}}{\frac{-V_{\mathrm{t5\text{-}n}}}{R_{\mathrm{t5}}} + I_{\mathrm{b\text{-}n}}}\right) \tag{22}$$

- Sequence 6, period t_6: In this sequence, no current flows in the inductor. The duration of this sequence can be calculated by:

$$t_{\mathrm{6\text{-}n}} = D_{\mathrm{n}}T_{\mathrm{s}} - (t_{\mathrm{4\text{-}n}} + t_{\mathrm{5\text{-}n}} + t_{\mathrm{7\text{-}n}}) \tag{23}$$

where, T_{s} is the switching period and D_{n} is the duty cycle during switching period n.

- Sequence 7, period t_7: The initial and final conditions are $I_{\mathrm{L7}}(t_{\mathrm{7i\text{-}n}}) = 0$ and $I_{\mathrm{L7\text{-}n}}(t_{7f-n}) = -I_{\mathrm{b\text{-}n}}$. Then:

$$I_{\mathrm{L7\text{-}n}} = \frac{V_{\mathrm{t7\text{-}n}}}{R_{\mathrm{t7}}}\left(1 - e^{\frac{-R_{\mathrm{t7}}}{L}t}\right) \tag{24}$$

The duration of this sequence is given by:

$$t_{\mathrm{7\text{-}n}} = \frac{-L}{R_{\mathrm{t7}}} \ln\left(1 + \frac{I_{\mathrm{b\text{-}n}}R_{\mathrm{t7}}}{V_{\mathrm{t7\text{-}n}}}\right) \tag{25}$$

- Sequence 8, period t_8: This is the second resonance period of the switching cycle in which the inductor resonates with the output capacitances of the main switches plus load capacitance. The initial and final conditions for this sequence are: $I_{\mathrm{L8}}(t_{\mathrm{8i\text{-}n}}) = -I_{\mathrm{b\text{-}n}}$, the initial voltage of the output capacitance $V_{\mathrm{Ci8}} = V_{\mathrm{dc}} - V_{\mathrm{fm1}}$ and final capacitance voltage $V_{\mathrm{Cf8}} = V_{\mathrm{onm}} + R_{\mathrm{onm}}i_{\mathrm{o\text{-}n}}$. The same procedure used in sequence 3 is followed to obtain the inductor current.
  The inductor current during the resonance mode is given by:

$$I_{\mathrm{L8\text{-}n}} = (2C_{\mathrm{m}} + C_{\mathrm{load}})\, e^{-\delta_8 t}(\lambda_{18}A_{\mathrm{8\text{-}n}}e^{j\omega_8 t} + \lambda_{28}B_{\mathrm{8\text{-}n}}e^{-j\omega_8 t}) + i_{\mathrm{o\text{-}n}} \tag{26}$$

The duration of this sequence is given by:

$$t_{\mathrm{8\text{-}n}} = \frac{\ln\left(\frac{(V_{\mathrm{Cf8}} - 0.5V_{\mathrm{dc}})}{2A_{\mathrm{8\text{-}n}}} + \sqrt{\frac{(V_{\mathrm{Cf8}} - 0.5V_{\mathrm{dc}})^2}{4A_{\mathrm{8\text{-}n}}^2} - \frac{B_{\mathrm{8\text{-}n}}}{A_{\mathrm{8\text{-}n}}}}\right)}{j\omega_8} \tag{27}$$

- Sequence 9, period t_9: The initial and final conditions are $I_{\mathrm{L9}}(t_{\mathrm{9i\text{-}n}}) = -I_{\mathrm{b\text{-}n}}$ and $I_{\mathrm{L9}}(t_{\mathrm{9f\text{-}n}}) = 0$. The inductor current is given by:

$$I_{\mathrm{L9\text{-}n}} = \frac{V_{\mathrm{t9\text{-}n}}}{R_{\mathrm{t9}}} + \left(I_{\mathrm{b\text{-}n}} - \frac{V_{\mathrm{t9\text{-}n}}}{R_{\mathrm{t9}}}\right) e^{\frac{-R_{\mathrm{t9}}}{L}t} \tag{28}$$

and the duration of this sequence is:

$$t_{\mathrm{9\text{-}n}} = \frac{-L}{R_{\mathrm{t9}}} \ln\left(\frac{\frac{-V_{\mathrm{t9\text{-}n}}}{R_{\mathrm{t9}}}}{I_{\mathrm{b\text{-}n}}} - \frac{V_{\mathrm{t9\text{-}n}}}{R_{\mathrm{t9}}}\right) \tag{29}$$

- Sequence 10, period t_{10}: In this sequence, no current flows in the inductor. The duration of this mode is given by:

$$t_{\mathrm{10\text{-}n}} = (1 - D_{\mathrm{n}})T_{\mathrm{s}} - (t_{\mathrm{3\text{-}n}} + t_{\mathrm{8\text{-}n}}) \tag{30}$$

TABLE I
SWITCHING SEQUENCES - USING MOSFETS

Sequence	M_1	M_2	A_1	A_2	Current eq. no.	Time eq. no.
1	Off	-CH	CH	-CH	5	6
2	Off	CH	CH	-CH	7	8
3	Off	Off	CH	-CH	15	18
4	-CH	Off	CH	-CH	19	20
5	CH	Off	CH	-CH	21	22
6	CH	Off	Off	Off	-	23
7	CH	CH	-CH	CH	24	25
8	Off	Off	-CH	CH	26	27
9	Off	-CH	-CH	CH	28	29
10	Off	-CH	Off	Off	-	30

TABLE II
R_{T} AND V_{T} FOR ALL SEQUENCES

Sequence	R_{t}	V_{t}
1	$R_{\mathrm{L}} + 2R_{\mathrm{ona}} + R_{\mathrm{onm2}}$	$0.5V_{\mathrm{dc}} + V_{\mathrm{xm2}}$
2	$R_{\mathrm{L}} + 2R_{\mathrm{ona}} + R_{\mathrm{onm2}}$	$0.5V_{\mathrm{dc}} - V_{\mathrm{xm2}}$
3	$R_{\mathrm{L}} + 2R_{\mathrm{ona}}$	see discussion
4	$R_{\mathrm{L}} + 2R_{\mathrm{ona1}} - R_{\mathrm{onm1}}$	$-0.5V_{\mathrm{dc}} - V_{\mathrm{xm1}}$
5	$R_{\mathrm{L}} + 2R_{\mathrm{ona1}} - R_{\mathrm{onm1}}$	$-0.5V_{\mathrm{dc}} + V_{\mathrm{xm1}}$
6	R_{onm1}	-
7	$R_{\mathrm{L}} + 2R_{\mathrm{ona}} - R_{\mathrm{onm1}}$	$-0.5V_{\mathrm{dc}} + V_{\mathrm{xm1}}$
8	$R_{\mathrm{L}} + 2R_{\mathrm{ona2}}$	see discussion
9	$R_{\mathrm{L}} + 2R_{\mathrm{ona2}} + R_{\mathrm{onm2}}$	$0.5V_{\mathrm{dc}} + V_{\mathrm{xm2}}$
10	R_{onm2}	-

B. Loss Calculation

From the duration and the inductor current of each mode, the losses in a single leg ARCPI are calculated as follows [6,7]:

- Sequence y:

$$E_{\mathrm{y\text{-}n}} = \int_0^{t_{\mathrm{y\text{-}n}}} ((R_{\mathrm{ty}}I_{\mathrm{Ly\text{-}n}} + V_{\mathrm{xm}})I_{\mathrm{Ly\text{-}n}})dt \tag{31}$$

where $y \in \{1, 4, 9\}$ and V_{xm} denotes the conducting main semiconductor based on Table I.

- Sequence x:

$$E_{\text{x-n}} = \int_0^{t_{\text{x-n}}} (R_{\text{tx}} I_{\text{Lx-n}}^2) dt \tag{32}$$

where $x \in \{2, 3, 5, 7, 8\}$.

- Energy losses in the resistance of the inductor L: As discussed above, the current flows in the inductor in all sequences except 6 and 10, so the energy lost in the inductor is given by (This energy is already included in (32) and (31).):

$$E_{\text{L-n}} = R_{\text{L}} \sum_{k=1}^{K} \int_0^{t_{\text{k-n}}} I_{\text{Lk-n}}^2 dt \tag{33}$$

- The energy losses in the commutation circuit are given by (This is driven from (32) and (31).):

$$E_{\text{commut-n}} = \sum_{k=1}^{K} E_{\text{k-n}} \tag{34}$$

where K in (33) and (34) is sequence number k and $k \in \{1, 2, 3, 4, 5, 7, 8, 9\}$.

- The energy losses in the main switches (conduction losses) are given by:

$$E_{\text{Main-n}} = \int_0^{t_{\text{6-n}}} V_{\text{xm}} i_{\text{o-n}} dt + \int_0^{t_{\text{10-n}}} V_{\text{xm}} i_{\text{o-n}} dt \tag{35}$$

- Switching losses of the two auxiliary switches (A_1 and A_2): Sequence 1 starts with M_2 conducting while A_1 blocks $0.5\,V_{\text{dc}}$. Thus, $V_{\text{ds-A}_1} = 0.5 V_{\text{dc}}$ and $V_{\text{ds-A}_2} = 0$. The turn on losses of the auxiliary switches equal the energy stored in the output capacitance of A_1 given by:

$$E_{\text{swon-n}} = \int_0^{0.5 V_{\text{dc}}} C_{\text{aux}}(v) v dv \tag{36}$$

During sequence 5, A_2 is turned off just before the zero crossing of the inductor current. This reduces the reverse recovery charge of the body diode. After the zero crossing A_1 is turned off. The reverse recovery of the body diode is divided into two intervals of equal length. During the first, the reverse current reaches its maximum, causing energy to be stored in the inductor yields:

$$E_{\text{Lr-n}} = \frac{L_{\text{r}} I_{\text{RM}}^2}{2} \tag{37}$$

The peak of this reverse current I_{RM} is estimated by:

$$V_{\text{Lr}} = L_{\text{r}} \frac{di}{dt} = L_{\text{r}} \frac{2 I_{\text{RM}}}{t_{\text{rr}}} \tag{38}$$

$$t_{\text{rr}} = \frac{2 L_{\text{r}} I_{\text{RM}}}{V_{\text{Lr}}} \tag{39}$$

where $V_{\text{Lr}} = 0.5\,V_{\text{dc}}$. Then I_{RM} is given by [based on [19]]:

$$I_{\text{RM}} = \sqrt{\frac{I_{\text{b-n}} Q_{\text{rr}} V_{\text{Lr}}}{L_{\text{r}} I_{\text{aux-n}}}} \tag{40}$$

where Q_{rr} is the reverse recovery charge mentioned in the data sheet and $I_{\text{aux-n}}$ is the nominal current of the auxiliary switches mentioned in the data sheet.
During the second part of the reverse recovery time, the reverse current decreases linearly to zero. Assuming linear voltage increase the energy dissipated in the switch is approximated by:

$$E_{\text{swoff-n}} = \int_0^{0.5 t_{\text{rr}}} I_{\text{R}}(t).V_{\text{ds}}(t) dt = I_{\text{RM}} V_{\text{ds-peak}} \frac{t_{\text{rr}}}{12} \tag{41}$$

The total switching losses of both auxiliary switches for both the positive and the negative period of the resonant current are given by:

$$E_{\text{sw-n}} = 2(E_{\text{swon-n}} + E_{\text{Lr-n}} + E_{\text{sw-off-n}}) \tag{42}$$

- The energy lost in the gate of the two main switches and the two auxiliary switches is given by:

$$E_{\text{gt-n}} = 2 Q_{\text{gt-main}} \frac{V_{\text{drm}}^2}{V_{\text{qgm}}} + 2 Q_{\text{gt-aux}} \frac{V_{\text{draux}}^2}{V_{\text{qgaux}}} \tag{43}$$

Q_{gt} is the total gate charge at a gate voltage of V_{qg} as given in the data sheet and driving voltage V_{dr}.

- Finally, to determine the total power losses in the single leg ARCPI, the energy lost in all components of the circuit is summed over N switching cycles within the positive half of the output current waveform ($0.5/f_{\text{mod}}$). This energy is then averaged over half of the fundamental period, where:

$$P_{\text{ARCPI}} = 2 f_{\text{mod}} \sum_{n=1}^{N} (E_{\text{Main-n}} + E_{\text{commut-n}} + E_{\text{sw-n}} + E_{\text{gt-n}}) \tag{44}$$

III. Main Circuit Component Selection

Switches from different families of (500 V - 650 V) MOSFETS (CoolMOSs, IR-MOSFETs, FREDFETs) and IGBTs have been investigated to select the best fitting devices for a range of DC link voltage from 50 V - 350 V at 20 kHz switching frequency.

Figure 2 shows the simulated total losses of the selected two combinations out of more than 190 combinations from different MOSFETs and IGBTs (at 10 % of nominal load conditions). Also, it shows that the homogeneous ARCPI (of which both the main and the auxiliary switches are MOSFETs [14]) has lower losses than the hybrid ARCPI (which has MOSFETs as main switches and IGBTs [15] for the auxiliary switches). Figure 3 shows the loss components of the homogeneous ARCPI for different DC link voltages $50\,\text{V} \leq V_{\text{dc}} \leq 350\,\text{V}$.

IV. Efficiency Enhancement

To improve the overall efficiency of the ARCPI, the contributions of each loss component were investigated separately.

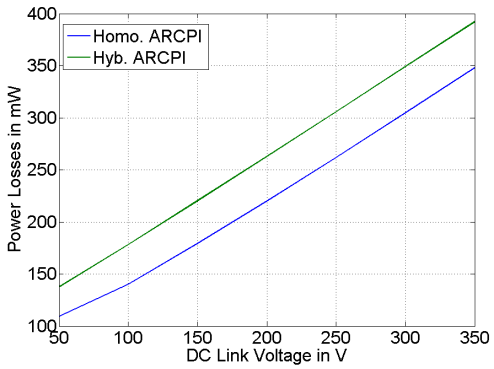

Fig. 2. Single leg ARCPI total losses for best two combinations. The homogeneous ARCP uses MOSFETs for both the main and the auxiliary switches [14] whereas the hybrid ARCPI uses MOSFETs [14] for the main switches and IGBTs for the auxiliary switches [15].

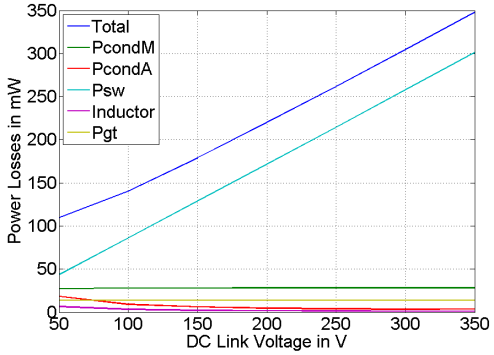

Fig. 3. Single leg loss components for the homogeneous ARCPI using MOSFETs (IPD65R1K4CFD2) [14].

1) Resistive Losses: As illustrated above in Figure 3, the conduction losses of the main (green curve) and the auxiliary switches (red curve) and the resistance losses in the inductor (pink curve) cannot be avoided because they are caused by the on state resistor of the switch, the internal resistance of the inductor and the load current.

2) Capacitive Losses: The switching losses of the auxiliary switches (cyan curve, Figure 3) are a combination of the discharging of the output capacitance of these switches (at turn on) and the energy stored in the inductor at turn off of the auxiliary switch and auxiliary switch turn off losses (42). Actually, in a conventional ARCPI, the auxiliary switches turn on and off at different times (per one switching cycle, one auxiliary switch per one resonant period). However, in this research, the auxiliary switches are turned on simultaneously. The turn off sequence of the auxiliary switches is optimized here: The reverse conducting auxiliary switch (A_2 in sequence 4) is turned off just before the zero crossing of the resonant inductor current, thus reducing the reverse recovery current and the associated losses. The second auxiliary switch is turned off after the zero crossing allowing for the oscillation to decay smoothly.

3) The RGD: The gate losses have a significant influence on the efficiency at low loads. Table III summarizes the gate losses for the cases of a homogeneous and a hybrid ARCPI.

TABLE III
COMPUTED GATE LOSSES, SINGLE ARCPI LEG.

ARCPI	Gate losses in mW
Homogeneous	13.59
Hybrid	61.06

In this research, the Resonant Gate Driving Circuit (RGD) proposed in [13], Figure 4 (left), has been employed to reduce the gate losses of the switches. To optimize the components of this circuit, it is important to select a low voltage MOSFET with a low on state resistor so as to reduce the conduction losses [13]. Also, the selection of the inductor L_r depends on its internal resistance, current rate and current capability [19].

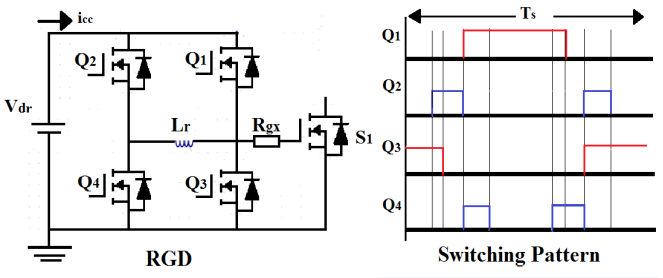

Fig. 4. The RGD (left) proposed in [13], switching pattern (right).

V. Discussion and Results

A. Test Circuit, Set up and Methods

Figure 1 (left) shows the test circuit to measure the losses. The circuit was built from one single leg. To reduce the ripple current and achieve nearly DC load current, a high inductor load was connected to the circuit. A variable DC-power supply provided the DC link voltage. As indicated in Figure 1 (left), the voltage and current input channels of a power analyzer [16] were connected to the input and the load of the single leg. This measurement setup is discussed in detail in [19].

B. Measurements and Discussion

Figure 5 shows the RGD prototype (left) together with the ARCPI prototype (right).

Figure 6 shows the measured load voltage (blue, scaled by $1/450$), input signal to the driver of A_1 (green, scaled by $1/10$) and resonant current (red), respectively. When A_1 is turned off (Figure 6, left), the inductor current decreases below zero and increases again to zero, whereas the negative peak of the current is caused by the reverse recovery charge of the body diode of A_2. Then, the current shows some oscillations due to the resonance between L_L and the output capacitances of the auxiliary switches before settling down to zero.

Figure 7 shows the measured losses combined with the computed losses of the single leg ARCPI (without gate losses).

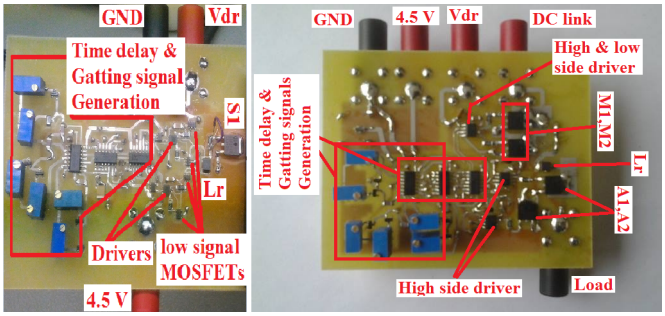

Fig. 5. The RGD prototype (left) and the ARCPI prototype (right).

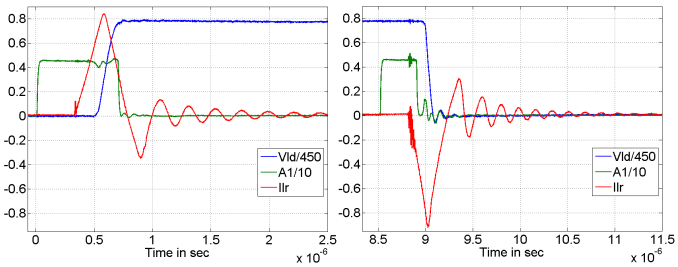

Fig. 6. Load voltage (blue scaled by 1/450), A_1 input voltage to A_1 driver (green scaled by 1/10), resonant current (red) at 350 V DC link voltage and 150 mA load current.

The comparison was done based on changing the DC link voltage when the load current is set to 150 mA (the peak value of the application).

In the case of hard switching, the use of the RGD increased the gate losses, because of the relative high switching speed needed to maintain low switching losses [19]. However, for soft switching, the switching speed of the switches can be reduced without compromising the switching losses, so the gate losses were reduced using the RGD.

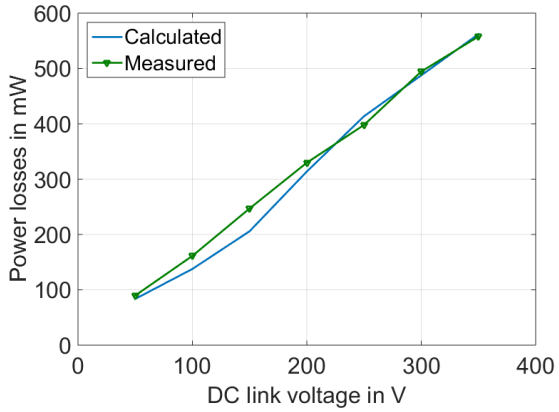

Fig. 7. Measured and computed ARCPI losses at a DC link voltages and DC load current of 150 mA

VI. Conclusions

This paper discussed the performance of a three phase soft switching inverter under an extremely light load (7 W, 50 V-peak and 150 mA-peak). This was 10 % of the maximum power of the appliance. An Auxiliary Resonant Commutated Pole Inverter (ARCPI) had been selected as a soft switching topology. The losses occurring in the inverter were discussed in detail. Also, the paper introduced two options to improve the inverter efficiency: First turning on the auxiliary switches at the same time which reduces the switching losses in the auxiliary switches. Second, the gate losses were reduced using an RGD.

Acknowledgment

This work has been carried out within the framework of ECO-COOL, a research project funded by FFG (Austrian Research Promotion Agency).

References

[1] M. H. Rashid, "Power Electronics HandBook", *Academic Press*, 2001.
[2] R.W. De Doncker and J.P. Lyons, "The Auxiliary Quasi-Resonant DC Link Inverter", *PESC 1991*, PP 248 - 253, June 1991.
[3] D. M. Divan, "The Resonant DC Link Converter- A New Concept in Static Power Conversion", *IEEE Transactions on Industry Applications*, Vol. 25, No. 2, March 1989.
[4] J.S. Lai, R.W. Young and J.W. McKeever, "Efficiency Consideration of DC Link Soft-Switching Inverters for Motor Drive Applications", *PESC 1994*, Vol.2, PP 1003 - 1010, June 1994.
[5] V. Pickert and C. M. Johnson, "An Assessment of Resonant Converters for Induction Motor Drives Applications up to 100 kW", *Power Electronics and Variable Speed Drives*, No. 429, September 1996.
[6] A. Cheriti, K. Al-Haddad, D. Mukhedkar, "Calculation of Power Loss in Soft Commutated PWM Inverters", *Industry Applications Society Annual Meeting*, Vol.1, PP 782 - 788, October 1991.
[7] A. Cheriti, K. Al-Haddad and L. A. Dessaint, "A Rugged Soft Commutated PWM Inverter for AC Drives", *IEEE Transactions on Power Electronics*, Vol. 7, No. 2, April 1992.
[8] Z. Y. Pan, F. L. Luo, "Novel Resonant Pole Inverter for Brushless DC Motor Drive System", *IEEE Transactions on Power Electronics*, Vol. 20, No. 1, January 2005.
[9] A. Toba, T. Shimizu, G. Kimura, "Auxiliary Resonant Commutated Pole Inverter Using Two Internal Voltage-Point of DC Source", *IEEE Transactions on Industrial Electronics*, Vol. 45, No. 2, April 1998.
[10] S. Karys, "Selection of Resonant Circuit Elements for ARCP Inverter", *10th International Conference on Electrical Power Quality and Utilization*, September, 2009.
[11] S. K. Pattnaik and K. K. Mahapatra, "Power Loss Estimation for PWM and Soft-Switching Inverter Using RDCLI", *IMECS 2010*, March 2010.
[12] E. Chu, M. Wu, L. Huang, X. Hou and H. Zhang, "Research on Novel Modulation Strategy for Auxiliary Resonant Commutated Pole Inverter with the Smallest Loss in Auxiliary Commutation Circuit", *IEEE Transactions on Power Electronics*, Vol. 29, No. 3, March 2014.
[13] W. Eberle, Y.F Liu and P.C Sen, "A New Resonant Gate-Drive Circuit with Efficient Energy Recovery and Low Conduction Loss", *IEEE Transactions on Industrial Electronics*, Vol. 55, No.5, May 2008.
[14] MOSFET, Data Sheet, Infineon Company, MOSFET type: IPD65R1400CFD2, http://www.infineon.com/.
[15] IGBT, Data Sheet, Infineon Company, IGBT type: IKD15N60RF, http://www.infineon.com/.
[16] Power Analyser data sheet, Fluke Norma 5000, http://www.transcat.com/media/pdf/FlukeNorma4K5K.pdf.
[17] P. Anthony and N. McNeill,"The efficient deployment of silicon superjunction MOSFETs as synchronous rectifiers", *PEMD 2014*, PP 1-6, April 2014.
[18] D. N. Pattanayak and O. G. Tornblad, "Large-Signal and Small-Signal Output Capacitances of Super Junction MOSFETs", *The 25th International Symposium on Power Semiconductor Devices and ICs*, Kanazawa.
[19] K. A. Mahafzah, K. Krischan and A. Muetze, "Efficiency Enhancement of a Three Phase Hard Switching Inverter Under Light Load Conditions", *IECON 16*, 6 pages, October 2016.